Journal of Bioscience and Bioengineering
VOL. 127 No. 1, 85–92, 2019

www.elsevier.com/locate/jbiosc

Pex16 is involved in peroxisome and Woronin body formation in the white koji fungus, *Aspergillus luchuensis* mut. *kawachii*

Daichi Kimoto,[1] Chihiro Kadooka,[1] Pakornkiat Saenrungrot,[1] Kayu Okutsu,[1] Yumiko Yoshizaki,[1] Kazunori Takamine,[1] Masatoshi Goto,[2] Hisanori Tamaki,[1] and Taiki Futagami[1,*]

Education and Research Center for Fermentation Studies, Faculty of Agriculture, Kagoshima University, 1-21-24 Korimoto, Kagoshima 890-0065, Japan[1] *and Department of Applied Biochemistry and Food Science, Faculty of Agriculture, Saga University, 1 Honjo-machi, Saga 840-8502, Japan*[2]

Received 1 April 2018; accepted 4 July 2018
Available online 27 July 2018

We characterized Pex16 in *Aspergillus luchuensis* mut. *kawachii* to examine the role of peroxisomes on citric acid production during the shochu-fermentation process. Rice koji made using a Δ*pex16* strain exhibited no significant change in citric acid accumulation but a 1.4-fold increase in formic acid production. Microscopic observation of mRFP-SKL (a peroxisome protein marker) showed that *pex16* disruption decreased the number of dot-like structures per hyphal cell to 5% of the control. Pex16-GFP exclusively co-localized with mRFP-SKL throughout the hyphae including the very close position to the septal pore. Moreover, the Δ*pex16* strain was hypersensitive to calcofluor white, which appeared to induce bursting of the hyphal tip and translocation of mRFP-SKL signals to the septal pore. These results indicate that Pex16 does not play a role in citric acid accumulation but is significantly involved in peroxisome and Woronin body formation in *Aspergillus kawachii*.

[**Key words:** *Aspergillus kawachii*; *pex16*; Peroxin; Peroxisome; Woronin body]

Aspergillus luchuensis mut. *kawachii* is a white koji fungus used for brewing shochu, a traditional Japanese alcoholic beverage (1–3). *Aspergillus kawachii* plays a significant role in the degradation of starch contained in ingredients such as barley, rice, buckwheat, and sweet potato into mono- or di-saccharides that can be further utilized by the yeast *Saccharomyces cerevisiae* for ethanol fermentation. In addition, *A. kawachii* produces a large amount of citric acid that prevents the growth of undesired microbes during the shochu-fermentation process.

The mechanism of citric acid overproduction has been extensively studied in *Aspergillus niger*, an organism used in the citric acid fermentation industry (4,5). Citric acid is synthesized as an intermediate of the tricarboxylic acid (TCA) cycle by citrate synthase in mitochondria and excreted to cytosol, and further to extracellular. For example, peroxisomal target signal 1 (PTS1) was also found at the C-terminus of mitochondrial citrate synthase, although citrate synthase activity was detected primarily in the mitochondrial fraction (6,7). In the case of *A. kawachii*, four citric acid synthase genes are present in the genome. The most highly expressed of these citrate synthase genes (locus tag: AKAW_06279) also encodes PTS1 in addition to the mitochondrial localization signal (8). Peroxisome-localized citrate synthase might be involved in the glyoxylate cycle (9,10). However, the functional role of the peroxisome in citric acid overproducing filamentous fungi remains to be determined.

In this study, we characterized a peroxin protein Pex16 required for peroxisome biogenesis to elucidate the relationship between the peroxisome and citric acid accumulation in *A. kawachii*. Pex16 is thought to play a significant role in the early stage of peroxisome assembly (11). The *pex16* gene is present in filamentous fungi, including those of the genus *Aspergillus*, but it is not present in most yeast, with the exception of *Yarrowia lipolytica*, which is a model citric acid producing organism (12,13). Data showing that disruption of *pex16* does not affect citric acid production by *A. kawachii* in koji suggest that the peroxisome does not play a significant role in citric acid accumulation during shochu fermentation. However, we further analyzed the functional role of *pex16* in *A. kawachii* and found that Pex16 is involved in peroxisome and Woronin body formation and required for functions such as long-chain fatty acid metabolism and tolerance to hyphal tip damage.

MATERIALS AND METHODS

Strains and growth conditions *A. kawachii* strains used in this study are listed in Table 1. The strains were grown at 30 °C in minimum medium (MM) (1% [wt/vol] glucose, 0.6% [wt/vol] $NaNO_3$, 0.052% [wt/vol] KCl, 0.052% [wt/vol] $MgSO_4 \cdot 7H_2O$, 0.152% [wt/vol] KH_2PO_4, 0.211% [wt/vol] arginine, and Hutner's trace elements [pH 6.5]). To test the ability to utilize carbon sources, 0.5% sodium oleate or 50 mM sodium acetate was added to the MM as a carbon source instead of glucose. Medium was adjusted to the required pH using NaOH. Antifungal agents were purchased from the following companies: Congo red and dithiothreitol, Nakalai Tesque (Kyoto, Japan); fluorescent brightener 28 (calcofluor white, CFW),

* Corresponding author. Education and Research Center for Fermentation Studies, Faculty of Agriculture, Kagoshima University, 1-21-24 Korimoto, Kagoshima 890-0065, Japan. Tel./fax: +81 99 285 3536.
E-mail address: futagami@chem.agri.kagoshima-u.ac.jp (T. Futagami).

1389-1723/$ – see front matter
https://doi.org/10.1016/j.jbiosc.2018.07.003

Sigma–Aldrich (St. Louis, MO, USA); menadione (2-methyl-1,4-naphthoquinone), Tokyo Chemical Industry (Tokyo, Japan).

Construction of *pex16*-disruptant strain *A. kawachii* ST2 served as the wild-type (wt) strain in this study (14). The *pex16* gene was disrupted in wt *A. kawachii* by insertion of the *argB* gene. A gene replacement cassette encompassing 2 kb at the 5′ end of *pex16*, 1.8 kb of *argB*, and 2 kb at the 3′ end of *pex16* was constructed by recombinant PCR using the primer pairs AKpex16-FC/AKpex16-R1, AKpex16-F2/AKpex16-R2, and AKpex16-F3/AKpex16-RC, respectively (Table S1). For amplification of the *argB* gene, the plasmid pDC1 was used as the template DNA (15). The resultant DNA fragment amplified with primers AKpex16-F1 and AKpex16-R3 was used to transform wt *A. kawachii*. For the selection of transformants, MM agar plates without arginine were used. Introduction of the *argB* gene into the *pex16* locus was confirmed by PCR using the primer pairs AKpex16-FC/AKpex16-R2 and AKpex16-F2/AKpex16-RC (Fig. S1A).

Complementation of the *pex16*-disruptant strain For analysis of complementation of the *pex16* disruptant with wt *pex16*, a gene replacement cassette encompassing 2 kb of the 5′ end of *pex16*, 1.4 kb of wt *pex16*, 4.2 kb of *sC*, and 2 kb of the 3′ end of *pex16* was constructed by recombinant PCR using the primer pairs AKpex16-FC/AKpex16comp-R1, AKpex16comp-F2/AKpex16comp-R2, and AKpex16comp-F3/AKpex16-RC, respectively (Table S1). The resultant DNA fragment amplified using the primer pair AKpex16-F1/AKpex16-R3 was used to transform the *pex16* disruptant. Transformants were selected on MM agar without methionine. Introduction of the wt *pex16* gene into the *pex16* disruptant was confirmed by PCR using the primer pairs AKpex16-FC/AKpex16comp-R2 and AKpex16comp-F2/AKpex16-RC (Fig. S1B). The amplicon by the primer pair of AKpex16-FC/AKpex16comp-R2 was sequenced using a 3500xl Genetic Analyzer (Thermo Fisher Scientific, Waltham, MA, USA) with the AKpex16-seq primer (Table S1) to confirm the presence of *pex16* in the complemented strain.

Construction of the pex16-GFP–tagged strain For analysis of Pex16 localization, a *pex16* gene *gfp*-tagged cassette encompassing 2 kb of the 5′ end of *pex16*, 1.4 kb of wt *pex16*, 0.7 kb of *gfp*, 1.8 kb of *argB*, and 2 kb of the 3′ end of *pex16* was constructed by recombinant PCR using primer pairs AKpex16-FC/AKpex16gfp-R1, AKpex16gfp-F2/AKpex16gfp-R2, AKpex16gfp-F3/AKpex16gfp-R3, and AKpex16gfp-F4/AK3pex16-RC, respectively (Table S1). The resultant DNA fragment amplified using primer pair AKpex16-F1/AKpex16-R3 was used to transform the wt strain. For amplification of the *gfp* gene, the plasmid pFNO3 was used as the template DNA (16). The transformants were selected on MM agar plates without arginine. Introduction of *gfp* and *argB* into the downstream locus of *pex16* was confirmed by PCR using the primer pair AKpex16-FC/AKpex16-R3 (Fig. S1C). The amplicon was sequenced using a 3500xl Genetic Analyzer (Thermo Fisher Scientific) with the AKpex16-seq primer (Table S1) to confirm the presence of the *gfp* fused *pex16* gene in the tagging strain.

Construction of the mRFP-SKL-expressing strain For analysis of peroxisome formation in wt *A. kawachii* and *pex16*-disruptant strains, the plasmid pGS-PgpdA-mRFP-SKL was constructed as follows. A 1.1-kb DNA fragment of the promoter sequence of the *gpdA* gene was amplified by PCR using pGS-PgpdA-Inf-F and pGS-PgpdA-Inf-R and cloned into the *Sal*I site of pGS (14) (Table S1), yielding pGS-PgpdA. Next, a 0.7-kb DNA fragment of mRFP-SKL was amplified by PCR using pGS-PgpdA-mRFP-SKL-Inf-F and pGS-PgpdA-mRFP-SKL-Inf-R and cloned into the *Sal*I site of pGS-PgpdA, yielding pGS-PgpdA-mRFP-SKL. For amplification of mRFP incorporating SKL, the plasmid pXDRFP4 was used as the template DNA (16). In addition, an In-Fusion HD cloning kit (Takara Bio USA, Mountain View, CA, USA) was used for cloning reactions. pGS-PgpdA-mRFP-SKL was used to transform the wt and *pex16*-disruptant strains. The transformants were selected on MM agar plates without methionine.

Microscopic observation of conidial heads To observe the conidial heads of the wt *A. kawachii* and Δ*pex16* strains, 2×10^4 conidia were inoculated on MM agar plates and cultivated at 37 °C for 6 days, after which they were observed using an SMZ1500 stereoscopic microscope (Nikon, Tokyo, Japan).

TABLE 1. *Aspergillus kawachii* strains used in this study.

Strain	Genotype	Source or reference
ST2	*ligD*::*ptrA argB*::*hph sC*$^-$	14
SO2	*ligD*$^-$ *argB*::*hph sC*$^-$	14
Δ*pex16*	*ligD*::*ptrA argB*::*hph sC*$^-$ *pex16*::*argB*	This study
CΔ*pex16*	*ligD*::*ptrA argB*::*hph sC*$^-$ *pex16*::*argB* *pex16*-sC	This study
pex16-gfp	*ligD*::*ptrA argB*::*hph sC*$^-$ *pex16*::*pex16-gfp-argB*	This study
mRFP-SKL	*ligD*::*ptrA argB*::*hph argB*$^+$ *sC*$^-$ pGS-PgpdA-mRFP-SKL	This study
Δ*pex16 mRFP-SKL*	*ligD*::*ptrA argB*::*hph sC*$^-$ *pex16*::*argB* pGS-PgpdA-mRFP-SKL	This study
pex16-gfp mRFP-SKL	*ligD*::*ptrA argB*::*hph sC*$^-$ *pex16*::*pex16-gfp-argB* pGS-PgpdA-mRFP-SKL	This study

Microscopic observation of localization of Pex16-GFP and mRFP-SKL To observe the localization of Pex16-GFP and mRFP-SKL, 6×10^5 conidia of the *A. kawachii* Pex16-GFP and/or mRFP-SKL expressing strains were inoculated into 3 ml of MM in a glass-bottom dish. The inoculated conidia were observed by DMI6000B inverted-type fluorescent microscope (Leica Microsystems, Wetzlar, Germany). After cultivation at 30 °C for 18 h, vegetative hyphae were further observed by the microscope. Image contrast was adjusted using LAS AF Lite software, ver. 2.3.0, build 5131 (Leica Microsystems). To evaluate the number of dot-like signals associated with mRFP-SKL, 100 cells from each of 3 independent cultivations were observed.

To observe the effect of CFW on the submerged hyphal tips of the wt *A. kawachii* strain, we inoculated 6×10^5 conidia into 3 ml of MM in a glass-bottom dish. After 18 h of incubation at 30 °C, CFW was added to the medium to a concentration of 20 μg/ml. Mycelia were immediately observed after addition of CFW using DMI6000B inverted-type fluorescent microscope (Leica Microsystems), and the observations were completed within 20 min. To evaluate the rate of localization of mRFP-SKL close to the septal pore, 100 septa of tip cells from each of 3 independent cultivations were observed.

Koji production and analysis of acidity and organic acids To investigate organic acid production during the koji-production process, wt *A. kawachii* and *pex16*-disruptant strains were grown on rice as previously described, with some modifications (17). Briefly, the polished rice was steamed, and 2×10^7 conidia were inoculated per 20 g of pre-steamed rice and incubated at 30 °C for 43 h.

For the analysis of acidity, 5 g of prepared koji was homogenized with 25 ml of water, and acidity was measured by acid-base titration. The samples were then filtered using 0.2-μm pore-size filters, and the organic acids were analyzed by HPLC on a Prominence HPLC system (Shimadzu, Kyoto, Japan) equipped with tandem Shim-pack SCR-102H columns (Shimadzu). *p*-Toluene sulfonic acid (4 mM) was used as the mobile phase at a flow rate of 0.8 ml/min. The column temperature was maintained at 50 °C. The eluent was mixed with 16 mM Bis-Tris/80 μM EDTA and analyzed using a CDD-10AVP conductivity detector (Shimadzu). Organic acids standards included α-ketoglutaric acid, citric acid, malic acid, succinic acid, lactic acid, and formic acid. These organic acids were selected for evaluating the quality of koji.

Analysis of conidiation efficiency Approximately 2×10^4 conidia were inoculated onto the center of an 84-mm MM agar plate. After the incubation, newly formed conidia were suspended in 0.01% (wt/vol) Tween 20 solution and counted using a hemocytometer. The mean and standard deviation of the number of conidia formed were determined from the results of 3 independently prepared agar plates.

Preparation of *A. kawachii* extracts and immunoblot analysis To investigate the expression of Pex16-GFP and mRFP-SKL, 2×10^8 conidia of *A. kawachii* strains were inoculated into 100 ml of MM. After cultivation at 30 °C with shaking at 140 rpm for 24 h, mycelia were harvested by filtration. To extract protein, 0.05 g of each cell pellet was dissolved in 0.6 ml of HK buffer (25 mM Tris–HCl [pH 7.5], 300 mM NaCl, 5 mM EDTA, 0.5% NP-40) and mechanically disrupted by bead beating for 3 cycles at 6.0 m/s for 40 s using a FastPrep 120 Cell Disrupter System (Thermo Savant, Carlsbad, CA, USA). The homogeneous suspension was centrifuged at 2200× *g* for 5 min at 4 °C, and the supernatant was recentrifuged at 21,880× *g* for 15 min at 4 °C. The supernatant was examined by immunoblot analysis. Protein concentrations were determined using the Bradford Protein Assay kit (Bio-Rad) with bovine serum albumin as the standard. The protein solution was mixed with SDS-PAGE sample buffer. After separation of proteins on 10% SDS-polyacrylamide gels followed by electroblotting onto polyvinylidene difluoride membranes, the expression of Pex16-GFP and mRFP-SKL was detected using anti-GFP antibody (Roche, Mannheim, Germany) and anti-RFP antibody (Medical and Biological Laboratories, Nagoya, Japan), respectively. Proteins were visualized using Chemi-Lumi One (Nakalai Tesque) according to the manufacturer's instructions.

RESULTS

In silico* identification of Pex16 in *A. kawachii BLASTP analysis using the amino acid sequence of human Pex16 as the search query identified one Pex16 homolog (locus tag: AKAW_03727) with 29% identity. The *A. kawachii* Pex16 showed BLASTP identities of 82% and 35% to the functionally characterized Pex16 of *Penicillium chrysogenum* and *Yarrowia lipolytica*, respectively (13,18). Phylogenetic analysis showed that *A. kawachii* Pex16 can be classified with Pex16 from filamentous fungi, including *P. chrysogenum* and other *Aspergillus* species (Fig. S2), perhaps due to the close phylogenetic relationship between the genera *Aspergillus* and *Penicillium* (19).

Colony formation in the *pex16* disruptant To explore the functional role of *pex16*, we constructed *A. kawachii* Δ*pex16*, *pex16*-

complemented (CΔ*pex16*), and *pex16-gfp* strains. We compared colony formation by these strains under various conditions (Fig. 1). The colony diameter of the Δ*pex16* strain was slightly smaller on MM compared with that of the wt strain at 30 and 37 °C (Fig. 1A). The Δ*pex16* strain did not show high-temperature sensitivity at 42 °C. In addition, the color of Δ*pex16* colonies became significantly paler than that of the wt strain at 37 °C, indicating that *pex16* is involved in conidia formation at 37 °C.

Next, we investigated the effect of carbon source on growth of the *A. kawachii* strains (Fig. 1B). The Δ*pex16* strain showed a slight growth deficiency but formed colonies on acetate medium. By contrast, the Δ*pex16* strain did not form colonies on MM containing oleate as the sole carbon source, suggesting that Pex16 plays a significant role in the assimilation of oleate.

We also investigated the role of *pex16* in stress tolerance of the *A. kawachii* strains in the presence of growth inhibitors, menadione (oxidative stress), dithiothreitol (endoplasmic reticulum stress), Congo red (cell wall stress resulting from binding to glucan), and CFW (cell wall stress resulting from binding to chitin) (Fig. 1C). Colony formation by the Δ*pex16* strain was not inhibited by menadione, dithiothreitol, or Congo red. By contrast, the Δ*pex16* strain produced significantly smaller colonies in the presence of CFW, indicating that *pex16* is involved in stress tolerance to CFW.

Complementation of *pex16* (CΔ*pex16*) successfully remedied the above-mentioned decrease in colony size in the Δ*pex16* strain. In addition, the *pex16-gfp* tagged strain showed a similar phenotype to the wt strain under all of the tested conditions (Fig. 1), suggesting that Pex16-GFP is functional in *A. kawachii*.

Conidia formation in the *pex16* disruptant As the difference in colony color indicated that disruption of *pex16* partially inhibited conidia formation on MM at 37 °C (Fig. 1A), we investigated conidia formation in greater detail (Fig. 2). Strains were cultivated on MM for 5 days, at which time the number of conidia formed was determined. The number of conidia formed per cm^2 by the Δ*pex16* strain did not change at 30 °C but declined significantly to 6% of the number produced by the wt strain cultured on MM at 37 °C (Fig. 2A).

To clarify whether the timing of differentiation into conidiophore was delayed in the Δ*pex16* strain at 37 °C, we measured the time-dependent conidia formation on MM agar plate at 37 °C (Fig. 3B). The number of conidia formed per cm^2 increased in the wt strain, whereas it remains to be reduced in the Δ*pex16* strain throughout the 14 days cultivation duration. These results indicated that *pex16* is significantly involved in conidia formation at 37 °C.

We also compared the conidial heads of the wt and Δ*pex16* strains after the cultivation at 37 °C for 6 days (Fig. 2C). Fewer conidial heads and a higher proportion in an immature state were observed in the Δ*pex16* strain. Thus, disruption of *pex16* appears to result in a decrease in the rate of hyphal differentiation into conidia. In particular, the maturation step after formation of vesicles appeared to be slower in the Δ*pex16* strain, based on microscopic observations (Fig. 2C).

Peroxisome formation in the *pex16* disruptant To elucidate the role of *pex16* in peroxisome formation in *A. kawachii*, we compared localization of the peroxisomal marker protein, mRFP-SKL (mRFP with a peroxisome localization signal), in the wt and Δ*pex16* strains (Fig. 3). Expression of mRFP-SKL was confirmed by immunoblot analysis based on a band of predicted molecular weight (Fig. S3, left panel).

In the wt strain, dot-like mRFP-SKL structures were apparent in the vegetative hyphae (Fig. 3A, left panel). By contrast, in the Δ*pex16* strain, signals were diffused throughout the hyphae. Next, we compared the number of dot-like structures per single hyphal cell between the wt and Δ*pex16* strains (Fig. 3B). We first evaluated the effect of *pex16* disruption on cell size. No significant difference in the distance between septa was observed between the wt and Δ*pex16* strains. In the Δ*pex16* strain, the number of dot-like structures per hyphal cell was significantly reduced (4% of that of the wt strain). These results indicated the Pex16 plays an important role in peroxisome formation during hyphal growth in *A. kawachii*.

Dot-like structures were also observed in the conidia of both the wt and Δ*pex16* strains (Fig. 3A, right panel). Interestingly, the number of dot-like structures did not change significantly between the wt and Δ*pex16* strains (Fig. 3B), indicating that *pex16* might not be required for peroxisome formation in the conidia.

Organic acid production in the *pex16* disruptant After confirming a reduction in the number of peroxisomes formed in the Δ*pex16* strain, we investigated organic acid production in rice koji, a

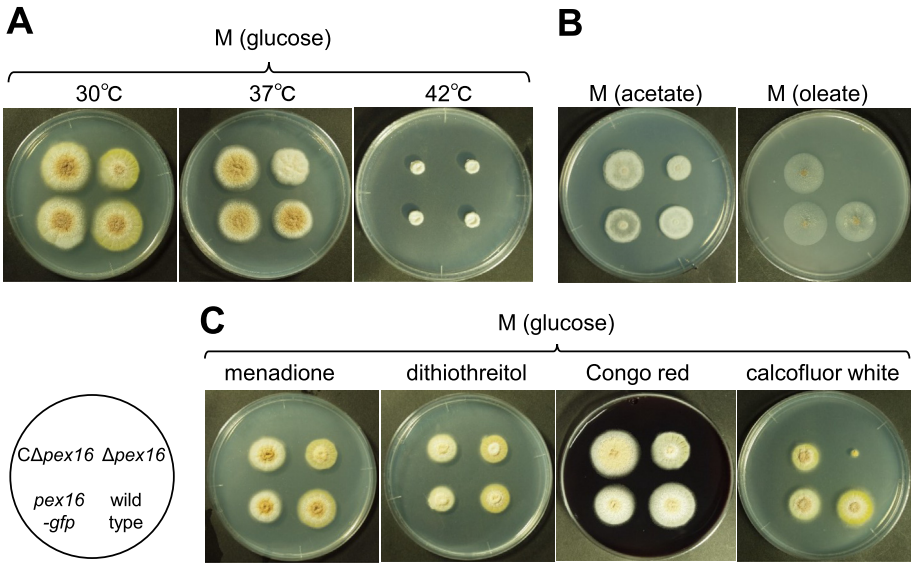

FIG. 1. Colony formation in wt *A. kawachii* and Δ*pex16*, CΔ*pex16*, and *pex16-gfp* strains. Strains were cultivated at different temperatures (30, 37, or 42 °C) for 5 days on MM containing glucose as the carbon source (A). For comparison of carbon source utilization, strains were cultivated on MM containing 0.5% sodium oleate or 50 mM sodium acetate as the carbon source instead of glucose at 30 °C for 5 days (B). To test stress tolerance, *A. kawachii* strains were cultivated at 30 °C for 6 days on MM (glucose) with 30 mM menadione, 8 mM DTT, 400 μg/ml Congo red, or 50 μg/ml CFW (C). Agar medium was inoculated with 2×10^4 conidiospores.

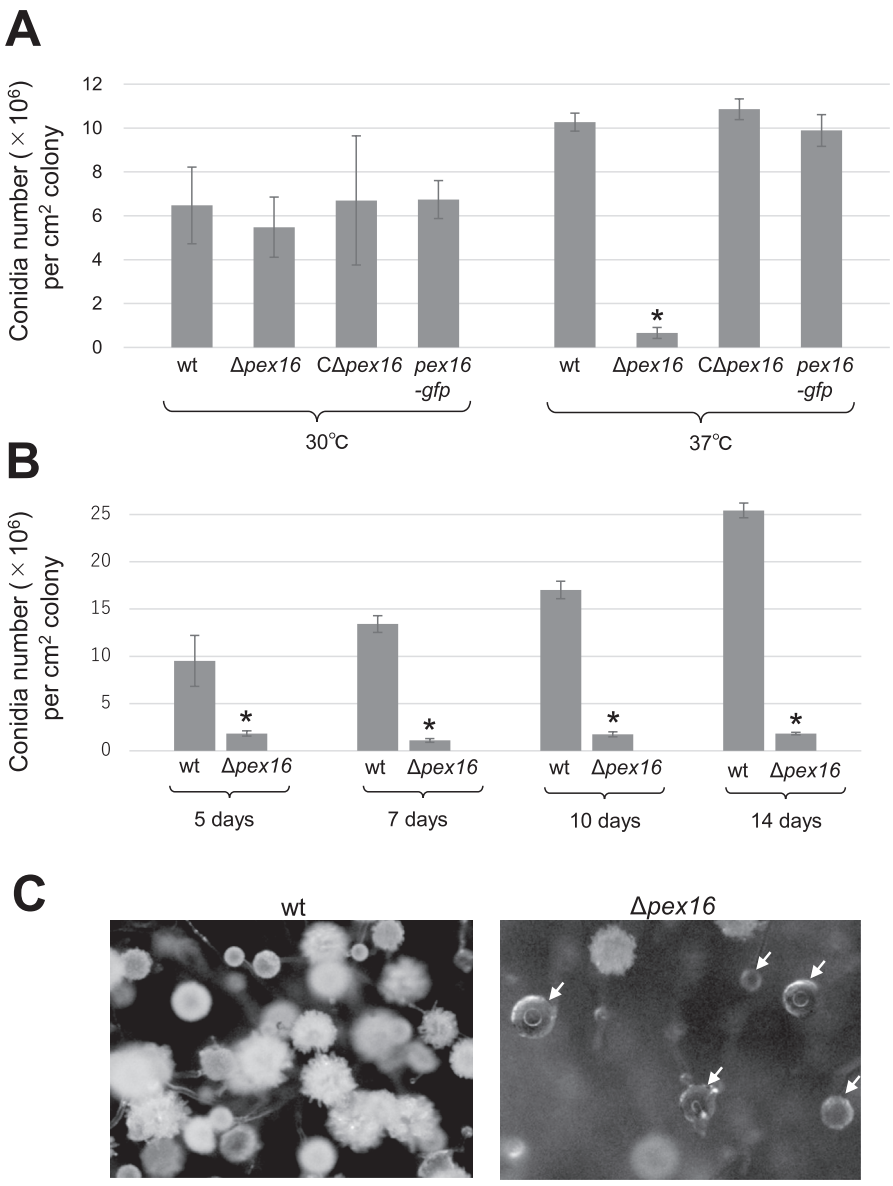

FIG. 2. Comparison of conidia formation in wt *A. kawachii* and Δ*pex16*, CΔ*pex16*, and *pex16-gfp* strains. Number of conidia formed by *A. kawachii* strains (A, B). The mean and the standard deviation were calculated from the results of 3 independent experiments. *Statistically significant difference ($p < 0.05$, Welch's *t*-test) relative to the result for the wt strain. Stereomicroscope observations of wt *A. kawachii* and Δ*pex16* strains (C). Arrows indicate immature conidial heads in the Δ*pex16* strain.

solid-state culture used in shochu brewing (Fig. 4). First, the acidity of the rice koji was measured to evaluate the accumulation of organic acids (Fig. 4A). The acidity of koji prepared using the Δ*pex16* strain was significantly higher than that of koji produced using the wt strain. Next, we assessed the organic acid composition of koji made using the wt and Δ*pex16* strains (Fig. 4B). No significant differences were observed in terms of the levels of α-ketoglutaric acid, citric acid, malic acid, succinic acid, and lactic acid (Fig. 4B), indicating that the peroxisome is not involved in production of these organic acids during rice koji production. However, the level of formic acid in rice koji made using the Δ*pex16* strain was 1.4-fold higher than that detected in rice koji made using the wt strain. This result was consistent with the higher acidity of rice koji prepared using the Δ*pex16* strain compared with that of rice koji prepared using the wt strain.

Localization of Pex16-GFP To investigate the localization of Pex16, we constructed a strain expressing GFP-tagged Pex16 (Fig. 5), in which *pex16-GFP* was expressed under control of the native *pex16* promoter. Expression of functional Pex16-GFP was confirmed based on similarity of phenotype with the wt strain (Fig. 1). In addition, expression of Pex16-GFP was confirmed by immunoblot analysis based on the presence of a band of predicted molecular weight (Fig. S3, right panel).

The Pex16-GFP signal was completely merged with that of mRFP-SKL, indicating that Pex16-GFP localized in the peroxisome (Fig. 5A). In addition, co-localization of Pex16-GFP and mRFP-SKL signals was observed in the area very close to the septal pore (Fig. 5B). Woronin bodies are peroxisome-derived organelles (20–22). This result indicates that Pex16-GFP localizes to both the peroxisome and Woronin body.

We also investigated the Pex16-GFP and mRFP-SKL signals during the differentiation stage using the MM slide culture at 30 °C (Fig. S4A, upper panel). The Pex16-GFP and mRFP-SKL signals were detected in the *pex16-gfp* strain, indicating that the Pex16 expressed during the conidia formation. However, it was difficult to

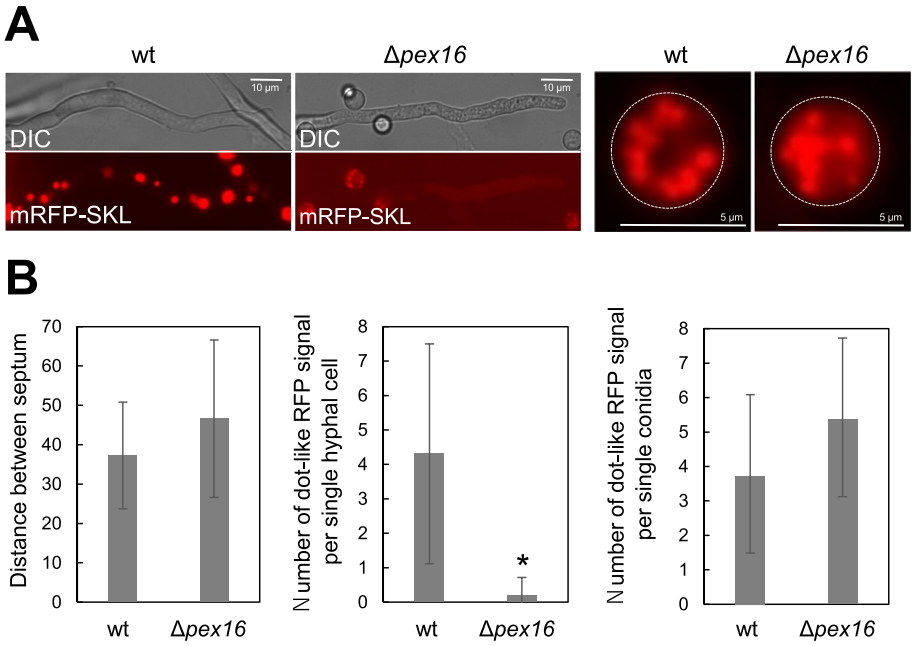

FIG. 3. Peroxisome formation in wt *A. kawachii* and Δ*pex16* strains. Fluorescent microscopic observation of mRFP-SKL expressed in wt and Δ*pex16* strains (A). Dashed lines indicate the outline of the conidia. Distance between septa and number of dot-like signals per hyphal cell and conidia (B). The mean and the standard deviation were calculated from the results of 3 independent experiments. *Statistically significant difference ($p < 0.05$, Welch's *t*-test) relative to the result for the wt strain.

observe the mRFP-SKL signal in the Δ*pex16* strain at the time after 3 days cultivation (Fig. S4A, lower panel). This was inconsistent with the previous observation that the number of mRFP-SKL signals was not changed significantly in conidia between the wt and Δ*pex16* strains (Fig. 3). Thus, we compared the signal intensity in the conidia retrieved after the different cultivation times (3, 5, and 7 days) on MM agar plate at 30 °C (Fig. S4B). The signal intensity of mRFP-SKL in the Δ*pex16* strain was significantly lower than that in the *pex16-gfp* strain, but increased by making the cultivation time longer (from 3 day to 5 and 7 days). These results indicated that formation of peroxisome structure in conidia might be delayed by the *pex16*-disruption.

Role of Pex16 in tolerance to CFW The greater sensitivity of the Δ*pex16* strain to CFW compared with the wt strain (Fig. 1C) suggests that *pex16* plays a significant role in tolerance to stress resulting from inhibition of chitin synthesis. In addition, disruption of *pex16* caused a reduction in the number of peroxisomes, which should subsequently cause a reduction in the number of Woronin bodies (Figs. 3 and 5). One role of the Woronin body is to seal the septal pore to prevent leakage of cytoplasm in response to hyphal damage (22). Thus, we hypothesized that the high sensitivity of the Δ*pex16* strain to CFW might be due to the combination of deficiency in Woronin body formation and CFW-induced hyphal tip bursting. To test this

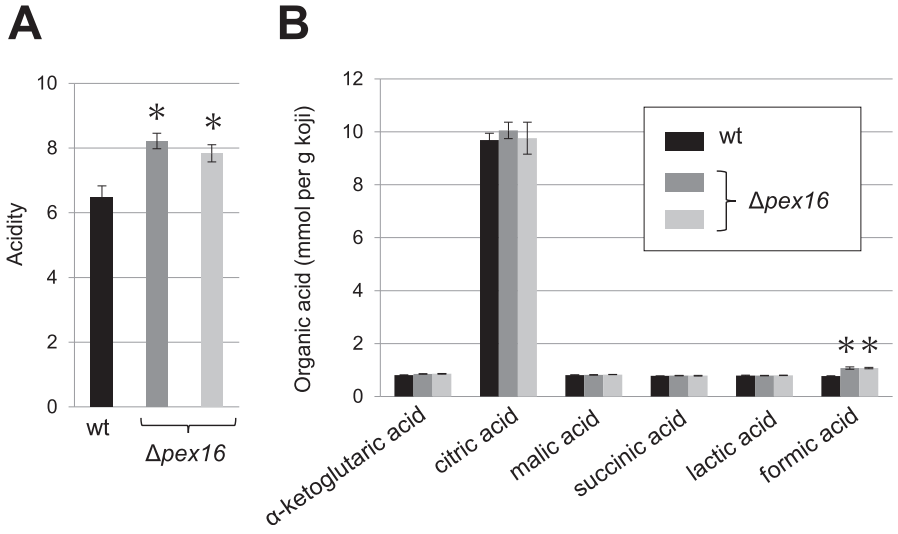

FIG. 4. Organic acid production in wt *A. kawachii* and Δ*pex16* strains used in rice koji. Acidity (A) and organic acid concentration (B) were measured for the wt strain and two *pex16* disruptants. The mean and the standard deviation were calculated from the results of 3 independent experiments. *Statistically significant difference ($p < 0.05$, Welch's *t*-test) relative to the result for the wt strain.

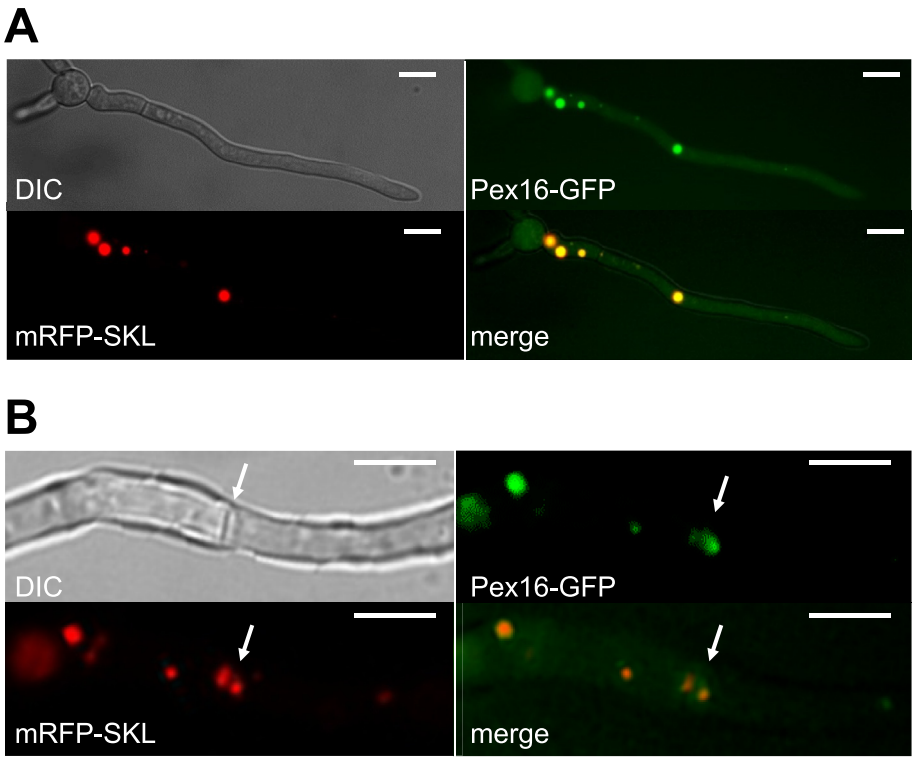

FIG. 5. Localization of Pex16-GFP in the *A. kawachii pex16-gfp* strain. Microscopic observation of a hyphal tip (A) and septum (B). Bar represents 10 μm. Arrows in panel B indicate position of the septum.

hypothesis, we first confirmed the appearance of hyphal tip bursting by treating with CFW, as shown in Fig. 6A. In addition, we confirmed an increase from 52% to 76% in mRFP-SKL signal intensity very close to the septum position of the tip cell after the treatment with CFW (Fig. 6B). These results supported our hypothesis, although it is possible that Pex16 might also be involved in maintaining cell wall integrity through an as yet unknown mechanism.

DISCUSSION

In this study, we characterized Pex16 homolog in *A. kawachii* as a means of assessing the relationship between the peroxisome and citric acid accumulation in *A. kawachii* used for shochu brewing. However, our results suggested that the observed reduction in peroxisome formation had no effect on citric acid productivity in the rice koji (Fig. 4). We found that level of formic acid in rice koji made

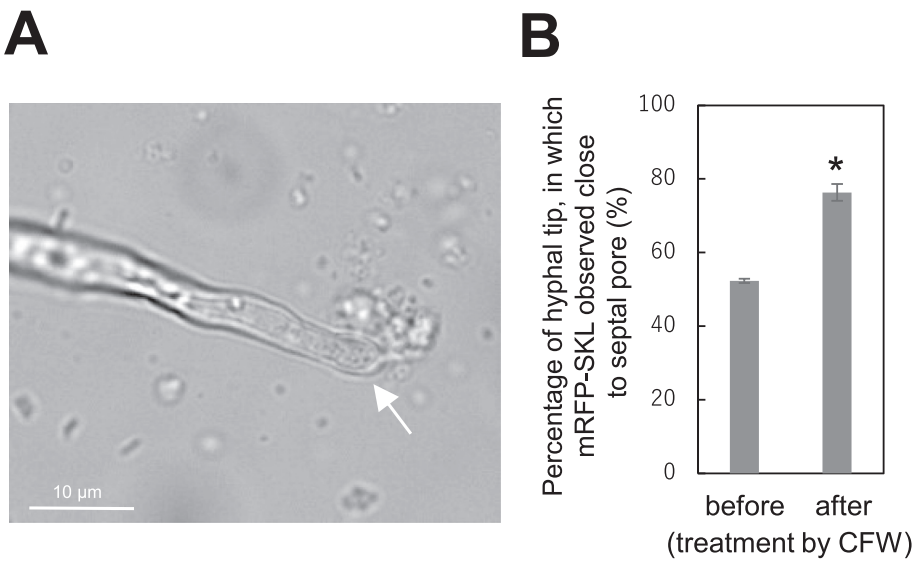

FIG. 6. Effect of CFW on *A. kawachii*. Microscopic observation of a hyphal tip after the addition of CFW to a culture of the wt strain (A). Arrow indicates leakage of cytoplasm from the tip. Percentage of hyphal tips in which mRFP-SKL was observed close to the septal pore (B). A total of 100 tip cell septa were observed before and after treating with CFW. The mean and standard deviation were calculated from the results of 3 independent experiments. *Statistically significant difference ($p < 0.05$, Welch's *t*-test) relative to the result before treatment with CFW.

using the Δ*pex16* strain was 1.4-fold higher than levels in rice koji made using the wt strain. Because formic acid can be converted into ester compounds producing a fruity type of flavor as a result of the heating process during distillation, the deficiency in peroxisome formation could affect the flavor of shochu, although it is unclear whether consumers prefer the flavor. For example, various esters of formic acid (e.g., isopropyl formate, ethyl formate, and methyl formate) have been identified in shochu and awamori, which is another Japanese distilled spirit made using rice koji (23,24).

A conceivable explanation for the accumulation of formic acid is increased rates of upstream reactions and/or reduced flux rates downstream in the metabolic pathways involved in formic acid production. Formic acid is synthesized in five metabolic pathways (25): (i) oxaloacetate degradation via oxalate, in which oxalate decarboxylase catalyzes decarboxylation of oxalate to produce formate and CO_2 (26); (ii) folic acid biosynthesis, in which guanosine triphosphate (GTP) cyclohydrolase I catalyzes hydrolysis of GTP to produce formate and 2-amino-4-hydroxy-6-(erythro-1,2,3-trihydroxypropyl)-dihydropteridine triphosphate (27); (iii) the folate one-carbon pool, in which 5-formyltetrahydrofolate deformylase catalyzes the hydrolysis of 10-formyltetrahydrofolate to produce formate and tetrahydrofolate (25); (iv) synthesis of zymosterol, in which cytochrome P450 (lanosterol 14A-demethylase, Erg11) converts lanosterol into formate and 4,4-dimethylcholesta-8,14,24-triene-3-ol (28); and (v) methanol metabolism, in which formaldehyde dehydrogenase catalyzes the dehydrogenation of formaldehyde to produce formate (29). By contrast, formic acid is degraded via two metabolic pathways: (i) oxidation of formic acid, in which formate oxidase catalyzes the oxidative degradation of formate to CO_2 (30); and (ii) the folate one-carbon pool, in which formate-dihydrofolate ligase catalyzes the ligation of formate and dihydrofolate to produce 10-formyltetrahydrofolate (27). Although it remains unclear which metabolic pathway mediates accumulation of formic acid in the Δ*pex16* strain, all of the genes encoding the above-mentioned formate-related enzymes are conserved in the genome of *A. kawachii* (locus tags: AKAW_08448 [oxalate decarboxylase], AKAW_06392 [GTP cyclohydrolase I], AKAW_05422 [5-formyltetrahydrofolate deformylase], AKAW_10210 and AKAW_02124 [Erg11], AKAW_09958 [formaldehyde dehydrogenase], AKAW_10339 [formate oxidase], and AKAW_02497 [formate-dihydrofolate ligase]). In addition, it should also be noted that the formate could be produced by the action of pyruvate-formate lyase in the denitrifying fungi, *Fusarium oxysporum* (31). However, the candidate gene encoding the pyruvate-formate lyase has not been identified in the genome of *A. kawachii*.

Disruption of *pex16* in *A. kawachii* caused a deficiency in the ability to utilize oleate (Fig. 1). This result was consistent with previous reports indicating that the peroxisome is required for the oxidation of long-chain fatty acids (9). For example, *Aspergillus nidulans* strains with mutations in the genes encoding the peroxins PexA (Pex1), PexF (Pex6), PexM (Pex13), PexC (Pex3), and PexE (Pex5) exhibit growth deficiency in medium containing oleic acid as the carbon source (32). In addition, *P. chrysogenum* with *pex16* disruption also exhibit growth deficiency in oleate medium (18).

The *A. kawachii* Δ*pex16* strain grew as well on acetate medium as it did on glucose medium (Fig. 1), indicating that the glyoxylate cycle is functional in this mutant even in the absence of peroxisomes, as previously reported in studies of peroxins in *A. nidulans* (32) and *S. cerevisiae* (33). As mislocalization of maleate synthase (an enzyme unique to the glyoxylate cycle) to the cytoplasm was not found to cause growth deficiency in acetate medium, peroxisomal localization of the enzyme is not required for an active glyoxylate cycle in *A. nidulans* (32,34,35). Thus, it is necessary to distinguish between peroxisome formation and the glyoxylate cycle when discussing the role of *pex16* on citric acid production in *A. kawachii*.

The mutation in the peroxin encoding *PEX22* is known to cause the high malate production in *S. cerevisiae* (36). The Pex22 is required for importing of peroxisomal proteins into the peroxisomal matrix, thereby the mislocalization of peroxisomal malate dehydrogenase Mdh3 to the cytosol resulted in the high malate production phenotype in the *PEX22* mutant. Although *A. kawachii* genome encodes the three *MDH3* homologous genes (Locus tags: AKAW_04056, AKAW_04204, and AKAW_10371), the expression products are predicted to localize to cytosol or mitochondria based on the amino acid sequences. Actually, the malate dehydrogenase activities were detected from cytosol and mitochondrial fractions in *A. nidulans* (37).

A reduction in the number of peroxisomes formed in the Δ*pex16* strain was confirmed by microscopic observations of the peroxisome marker protein mRFP-SKL. The dot-like signals associated with mRFP-SKL did not completely disappear but were reduced to 5% of the wt level by disruption of *pex16* (Fig. 3). This result was in good agreement with a previous report describing the structure of peroxisomes in a *P. chrysogenum pex16* disruptant in which GFP-SKL was analyzed using fluorescence microscopy and electron microscopy (18). In addition, the number of mRFP-SKL signals in the conidia of both wt *A. kawachii* and the Δ*pex16* strains was comparable, suggesting that Pex16 is not required for peroxisome formation in the conidia.

In addition, mRFP-SKL localized very close to the septal pore with Pex16-GFP, indicating that Pex16 localizes not only in the peroxisome but also in the Woronin body, which would be expected, given that the Woronin body is derived from the peroxisome (20–22). For example, disruption of *pex11* was shown to lead to the disappearance of Woronin bodies in *Aspergillus oryzae* (38). The Woronin body plays a significant role in sealing the septal pore to prevent leakage of cytoplasm following hyphal damage. Because the *A. kawachii* Δ*pex16* strain was more sensitive to CFW than the wt strain (Fig. 1), we hypothesized that the reduced number of Woronin bodies in the Δ*pex16* strain was the cause of low tolerance to CFW that can cause hyphal tip bursting (Fig. 6). This hypothesis was supported by the observed increased localization of mRFP-SKL close to the septal pore following treatment with CFW.

In conclusion, the peroxin protein Pex16 plays a significant role in peroxisome and Woronin body formation during hyphal growth of *A. kawachii*, but it does not play a similar role in the conidia. The peroxisome deficiency in the Δ*pex16* strain coincided with an inability to utilize oleic acid, but not acetate, indicating that the glyoxylate cycle is still active in the Δ*pex16* strain. The peroxisome is not involved in citric acid production during the koji-production process in *A. kawachii*; instead, it is important in the formic acid metabolic pathway. Moreover, Woronin body deficiency in the Δ*pex16* strain appears to be associated with sensitivity to CFW. This is the first study to investigate the functional role of Pex16 in the genus *Aspergillus*.

Supplementary data related to this article can be found at https://doi.org/10.1016/j.jbiosc.2018.07.003.

ACKNOWLEDGMENTS

We thank Risako Uchimura and Kyoko Hori for technical support. This work was supported by a JSPS KAKENHI grant (no. 16K07672). The authors declare that there is no conflict of interest.

References

1. **Yamada, O., Takara, R., Hamada, R., Hayashi, R., Tsukahara, M., and Mikami, S.:** Molecular biological researches of Kuro-Koji molds, their classification and safety, J. Biosci. Bioeng., **112**, 233–237 (2011).
2. **Hong, S. B., Lee, M., Kim, D. H., Varga, J., Frisvad, J. C., Perrone, G., Gomi, K., Yamada, O., Machida, M., Houbraken, J., and Samson, R. A.:** *Aspergillus luchuensis*, an industrially important black *Aspergillus* in East Asia, PLoS One, **8**, e63769 (2013).
3. **Hong, S. B., Yamada, O., and Samson, R. A.:** Taxonomic re-evaluation of black koji molds, Appl. Microbiol. Biotechnol., **98**, 555–561 (2014).
4. **Karaffa, L. and Kubicek, C. P.:** *Aspergillus niger* citric acid accumulation: do we understand this well working black box? Appl. Microbiol. Biotechnol., **61**, 189–196 (2003).
5. **Legisa, M. and Mattey, M.:** Changes in primary metabolism leading to citric acid overflow in *Aspergillus niger*, Biotechnol. Lett., **2**, 181–190 (2007).
6. **Jaklitsch, W. M., Kubicek, C. P., and Scrutton, M. C.:** Intracellular location of enzymes involved in citrate production by *Aspergillus niger*, Can. J. Microbiol., **37**, 823–827 (1991).
7. **Ruijter, G. J., Panneman, H., Xu, D., and Visser, J.:** Properties of *Aspergillus niger* citrate synthase and effects of *citA* overexpression on citric acid production, FEMS Microbiol. Lett., **184**, 35–40 (2000).
8. **Futagami, T., Mori, K., Wada, S., Ida, H., Kajiwara, Y., Takashita, H., Tashiro, K., Yamada, O., Omori, T., Kuhara, S., and Goto, M.:** Transcriptomic analysis of temperature responses of *Aspergillus kawachii* during barley koji production, Appl. Environ. Microbiol., **81**, 1353–1363 (2015).
9. **Kunze, M., Pracharoenwattana, I., Smith, S. M., and Hartig, A.:** A central role for the peroxisomal membrane in glyoxylate cycle function, Biochim. Biophys. Acta, **1763**, 1441–1452 (2006).
10. **van der Klei, I. J. and Veenhuis, M.:** The versatility of peroxisome function in filamentous fungi, Subcell Biochem., **69**, 135–152 (2013).
11. **Kim, P. K. and Mullen, R. T.:** PEX16: a multifaceted regulator of peroxisome biogenesis, Front. Physiol., **4**, 241 (2013).
12. **Kiel, J. A., Veenhuis, M., and van der Klei, I. J.:** PEX genes in fungal genomes: common, rare or redundant, Traffic, **7**, 1291–1303 (2006).
13. **Cavallo, E., Charreau, H., Cerrutti, P., and Foresti, M. L.:** *Yarrowia lipolytica*: a model yeast for citric acid production, FEMS Yeast Res., **17**, fox084 (2017).
14. **Kadooka, C., Onitsuka, S., Uzawa, M., Tashiro, S., Kajiwara, Y., Takashita, H., Okutsu, K., Yoshizaki, Y., Takamine, K., Goto, M., Tamaki, H., and Futagami, T.:** Marker recycling system using the *sC* gene in the white koji mold, *Aspergillus luchuensis mut.* kawachii, J. Gen. Appl. Microbiol., **62**, 160–163 (2016).
15. **Aramayo, R., Adams, T. H., and Timberlake, W. E.:** A large cluster of highly expressed genes is dispensable for growth and development in *Aspergillus nidulans*, Genetics, **122**, 65–71 (1989).
16. **Yang, L., Ukil, L., Osmani, A., Nahm, F., Davies, J., De Souza, C. P., Dou, X., Perez-Balaguer, A., and Osmani, S. A.:** Rapid production of gene replacement constructs and generation of a green fluorescent protein-tagged centromeric marker in *Aspergillus nidulans*, Eukaryot. Cell, **3**, 1359–1362 (2004).
17. **Shiraishi, Y., Yoshizaki, Y., Ono, T., Yamato, H., Okutsu, K., Tamaki, H., Futagami, T., Sameshima, Y., and Takamine, K.:** Characteristic odour compounds in shochu derived from rice koji, J. Inst. Brew., **122**, 381–387 (2016).
18. **Opaliński, Ł., Bartoszewska, M., Fekken, S., Liu, H., de Boer, R., van der Klei, I., Veenhuis, M., and Kiel, J. A.:** De novo peroxisome biogenesis in Penicillium chrysogenum is not dependent on the Pex11 family members or Pex16, PLoS One, **7**, e35490 (2012).
19. **Samson, R. A., Visagie, C. M., Houbraken, J., Hong, S. B., Hubka, V., Klaassen, C. H., Perrone, G., Seifert, K. A., Susca, A., Tanney, J. B., and other 5 authors:** Phylogeny, identification and nomenclature of the genus *Aspergillus*, Stud. Mycol., **78**, 141–173 (2014).
20. **Jedd, G. and Chua, N. H.:** A new self-assembled peroxisomal vesicle required for efficient resealing of the plasma membrane, Nat. Cell Biol., **2**, 226–231 (2000).
21. **Tenney, K., Hunt, I., Sweigard, J., Pounder, J. I., McClain, C., Bowman, E. J., and Bowman, B. J.:** Hex-1, a gene unique to filamentous fungi, encodes the major protein of the Woronin body and functions as a plug for septal pores, Fungal Genet. Biol., **31**, 205–217 (2000).
22. **Maruyama, J. and Kitamoto, K.:** Expanding functional repertoires of fungal peroxisomes: contribution to growth and survival processes, Front. Physiol., **4**, 177 (2013).
23. **Yoshizaki, Y., Yamato, H., Takamine, K., Tamaki, H., Ito, K., and Sameshima, Y.:** Analysis of volatile compounds in shochu koji, sake koji, and steamed rice by gas chromatography-mass spectrometry, J. Inst. Brew., **116**, 49–55 (2010).
24. **Taira, J., Tsuchiya, A., and Furudate, H.:** Initial volatile aroma profiles of young and aged awamori shochu determined by GC/MS/pulsed FPD, Food Sci. Technol. Res., **18**, 177–181 (2012).
25. **Andersen, M. R., Nielsen, M. L., and Nielsen, J.:** Metabolic model integration of the bibliome, genome, metabolome and reactome of *Aspergillus niger*, Mol. Syst. Biol., **4**, 178 (2008).
26. **Emiliani, E. and Riera, B.:** Enzymatic oxalate decarboxylation in *Aspergillus niger*: II. Hydrogen peroxide formation and other characteristics of the oxalate decarboxylase, Biochim. Biophys. Acta, **167**, 414–421 (1968).
27. **Cossins, E. A. and Chen, L.:** Folates and one-carbon metabolism in plants and fungi, Phytochemistry, **45**, 437–452 (1997).
28. **van den Brink, H. J., van Nistelrooy, H. J., de Waard, M. A., van den Hondel, C. A., and van Gorcom, R. F.:** Increased resistance to 14 alpha-demethylase inhibitors (DMIs) in *Aspergillus niger* by coexpression of the *Penicillium italicum* eburicol 14 alpha-demethylase (*cyp51*) and the *A. niger* cytochrome P450 reductase (*cprA*) genes, J. Biotechnol., **49**, 13–18 (1996).
29. **Lusta, K. A., Sysoev, O. V., and Sharyshev, A. A.:** Cytobiochemical characterization of *Aspergillus terreus* 17p utilizing various carbon substrates, J. Basic Microbiol., **31**, 265–277 (1991).
30. **Hauge, J. G.:** Formic acid oxidation in *Aspergillus niger*, Biochim. Biophys. Acta, **25**, 148–155 (1957).
31. **Kuwasaki, S., Takaya, N., Nakamura, A., and Shoun, H.:** Formate-forming fungal catabolic pathway to supply electron to nitrate respiration, Biosci. Biotechnol. Biochem., **67**, 937–939 (2003).
32. **Hynes, M. J., Murray, S. L., Khew, G. S., and Davis, M. A.:** Genetic analysis of the role of peroxisomes in the utilization of acetate and fatty acids in *Aspergillus nidulans*, Genetics, **178**, 1355–1369 (2008).
33. **Erdmann, R., Veenhuis, M., Mertens, D., and Kunau, W. H.:** Isolation of peroxisome-deficient mutants of *Saccharomyces cerevisiae*, Proc. Natl. Acad. Sci. USA, **86**, 5419–5423 (1989).
34. **Gainey, L. D., Connerton, I. F., Lewis, E. H., Turner, G., and Balance, D. J.:** Characterization of the glyoxysomal isocitrate lyase genes of *Aspergillus nidulans (acuD)* and *Neurospora crassa (acu-3)*, Curr. Genet., **21**, 43–47 (1992).
35. **Szewczyk, E., Andrianopoulos, A., Davis, M. A., and Hynes, M. J.:** A single gene produces mitochondrial, cytoplasmic, and peroxisomal NADP-dependent isocitrate dehydrogenase in *Aspergillus nidulans*, J. Biol. Chem., **276**, 37722–37729 (2001).
36. **Negoro, H., Sakamoto, M., Kotaka, A., Matsumura, K., and Hata, Y.:** Mutation in the peroxin-coding gene *PEX22* contributing to high malate production in *Saccharomyces cerevisiae*, J. Biosci. Bioeng., **125**, 211–217 (2018).
37. **Osmani, S. A. and Scrutton, M. C.:** The sub-cellular localisation of pyruvate carboxylase and of some other enzymes in *Aspergillus nidulans*, Eur. J. Biochem., **133**, 551–560 (1983).
38. **Escaño, C. S., Juvvadi, P. R., Jin, F. J., Takahashi, T., Koyama, Y., Yamashita, S., Maruyama, J., and Kitamoto, K.:** Disruption of the Ao*pex11-1* gene involved in peroxisome proliferation leads to impaired Woronin body formation in *Aspergillus oryzae*, Eukaryot. Cell, **8**, 296–305 (2009).